Siberian Lidar Station – the unique experimental complex for remote investigations of the ozonosphere

V.V. Zuev

Institute of Atmospheric Optics,
Siberian Branch of the Russian Academy of Sciences, Tomsk

Received December 29, 1999

The Siberian Lidar Station (SLS) of the Institute of Atmospheric Optics SB RAS (Tomsk) is described in the paper. The results of long-term optical monitoring of the ozonosphere at the SLS are generalized and reviewed.

Dynamic variations of the stratospheric ozone layer (ozonosphere) attract the unremitting attention of researchers in the last decades. Successful development of the experimental basis of the Institute of Atmospheric Optics allowed us to create in the eighties powerful stationary lidars for remote sensing of the stratosphere and lower mesosphere. The first lidar with a mirror telescope of 1-m diameter and 2-m focal length was created in 1985. All the optical and mechanical components of the telescope, including its big primary mirror, were designed and manufactured at the Special Design Bureau "Optika." The lidar was deployed in a reconstructed premise. Regular observations of the stratospheric aerosol by means of this lidar started in 1986, and the first profiles of the stratospheric ozone were acquired in 1989 using its modified version.[1]

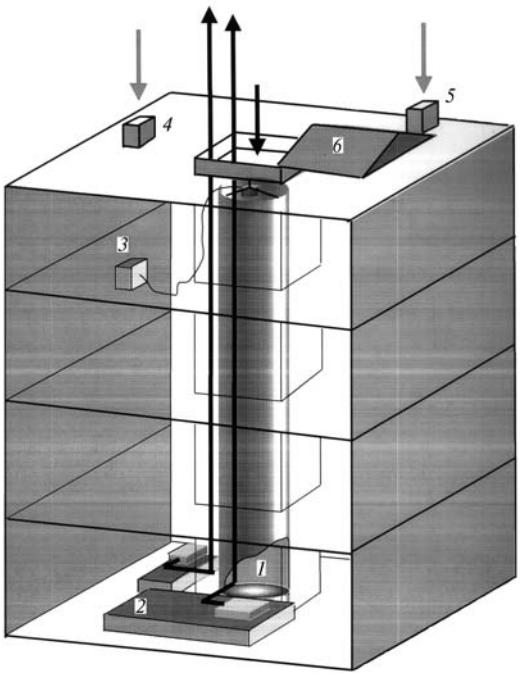

Fig. 1. SLS building with the primary mirror of the telescope deployed in the shaft. (*1*) 2.2-m-diameter mirror; (*2*) laser benches; (*3*) receiving-recording instrumentation; (*4*) M–124 ozonometer; (*5*) twilight spectrophotometer; and (*6*) movable roof of the shaft.

The larger receiving mirror of 2.2-m diameter and 10-m focal length was manufactured for the second lidar complex by special order at the Lytkarino optical-mechanical enterprise, and coated with a reflecting aluminum layer at the Leningrad optical-mechanical association. All other details of the receiving telescope were manufactured at the Special Design Bureau "Optika." The telescope was deployed in the shaft at the center of 4-storied building that was specially built for this lidar complex not far from the first stationary lidar. The telescope mirror was mounted at the ground floor level (Fig. 1). The principal benches with laser sources were installed at the same floor. Recording of lidar returns was performed in the focal plane of the mirror at the level of the 3rd floor.

The first signals were recorded with this lidar complex in 1990. Figure 2 shows an example of typical lidar return recorded at the wavelength of 532 nm of the second harmonic of a solid-state Nd:YAG laser.[2] It is seen that the potential capability of the lidar complex provides for acquiring data from atmospheric layers up to the height about 80 km.

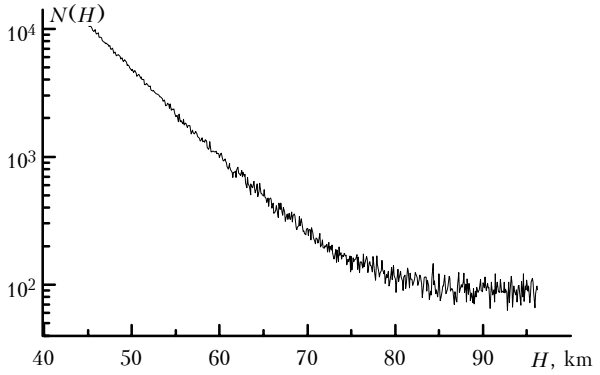

Fig. 2. Lidar return signal recorded at SLS up to the height of 80 km.

The Siberian Lidar Station (SLS) was formed on the basis of two stationary lidar complexes. After search for the optimal structure of the SLS, the pattern of lidar channels is realized now as is shown in Fig. 3. The specifications of these channels are presented in Table 1.

0235-6880/00/01 84-05 $02.00 © 2000 Institute of Atmospheric Optics

Table 1. Specifications of the SLS lidar channels

Parameters of the lidar	Measured characteristics					
	Ozone			Aerosol	Temperature	
Primary mirror diameter, m	2.2	1	0.3	0.5	2.2	1
Focal length, m	10	2	1.5	1.5	10	2
Wavelength of sensing, nm	308/353	308/353	308/353	532; 683	532	353 (384)
Pulse energy, mJ	80/20	80/20	80/20	100; 50	100	20
Pulse repetition rate, Hz	50–200	50–200	50–200	20	20	50–200
Height range of sensing, km	30–60	15–40	6–15	10–30	30–60	15–40 (3–15)
Maximum measurement error , %	10	10	15	7	±5 K	±3 K (±5 K)

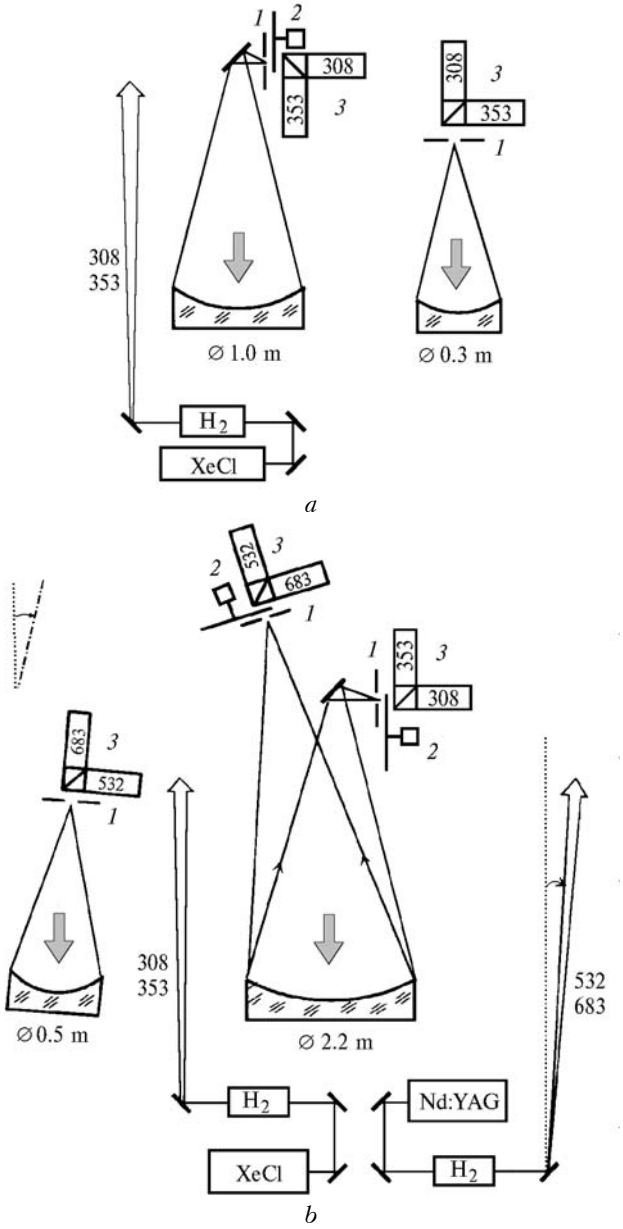

Fig. 3. The up-to-date block-diagram of the lidar channels at the SLS: lidar complex with a 1-m-diameter receiving mirror (*a*); lidar complex with a 2.2-m-diameter receiving mirror (*b*); field-stop diaphragm (*1*); mechanical chopper of the short-distance zone (*2*); block for the spectral selection of the PMT signals (*3*); XeCl is an excimer laser; Nd:YAG is the solid-state laser; H_2 is the stimulated Raman scattering cell with hydrogen.

The laser sources emitting at the wavelengths in the UV (excimer XeCl-lasers) and visible (Nd:YAG-laser) spectral ranges are used as transmitters of sounding radiation in the lidars operated in the parallel. The telescopes of smaller diameters, 0.5 and 0.3 m, are used in addition to the big telescopes. The long-focus telescope with 2.2-m-diameter mirror provides recording of lidar returns in the height range 30 to 60 km, the telescope with 1-m mirror operates in the range 15 to 40 km, the telescope with 0.5-m mirror operates in the range 10 to 30 km, and, finally, the telescope with 0.3-m mirror operates in the range 6 to 15 km. The signals from the atmospheric layers lower than the noted height ranges are cut off actively by means of a mechanical chopper or passively due to the big distance between the transmitter and a receiver.

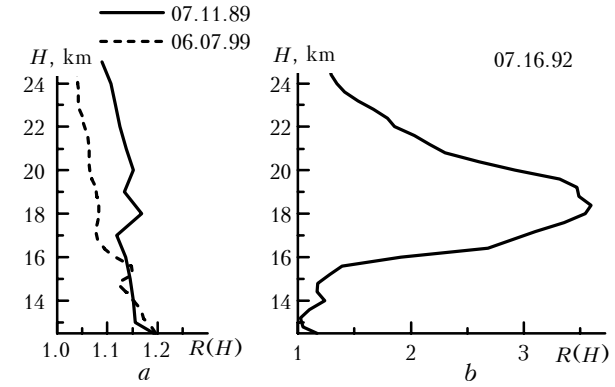

Fig. 4. Vertical profiles of the scattering ratio (ratio of the sum of the molecular and aerosol backscattering coefficients to the molecular backscattering coefficient) at the wavelength of 532 nm for the background (*a*) and perturbed (*b*) state of the stratospheric aerosol layer.

Capabilities of the SLS laser channels for remotely determining the vertical distribution of aerosol (VDA), ozone (VDO), temperature (VDT) are illustrated in Figs. 4, 5, and 6, respectively. The techniques for determining these characteristics are described in detail in Refs. 3–5. One should emphasize that it is possible to estimate the size of aerosol particles when operating in the mode of double- or triple-frequency sensing. In the simplest case of double-frequency sensing one can qualitatively analyze the particle size distribution by the behavior of the Angström parameter X (Fig. 7). As a rule, the less values X correspond to the aerosol particles of a bigger size. This example characterizes, on

the one hand, the process of sedimentation of aerosol particles with localization of the coarse fraction over the tropopause, and, on the other hand, the well-pronounced Junge layer formation. If operating in the triple-frequency mode, one can solve a more complicated problem of reconstructing the particle size spectrum.[6]

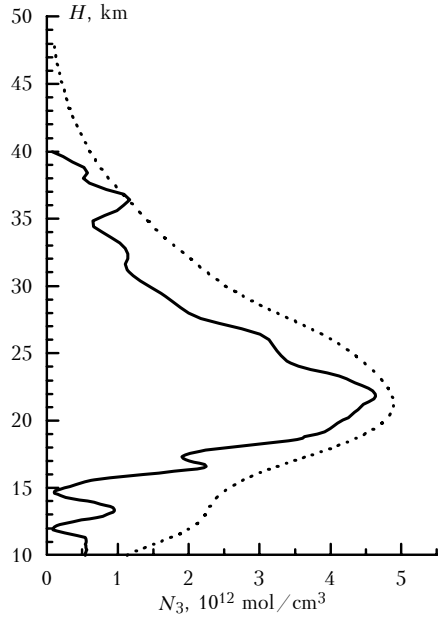

Fig. 5. Vertical profile of the ozone (solid line) measured on November 20, 1999 as compared with the Krueger model[21] (dotted line).

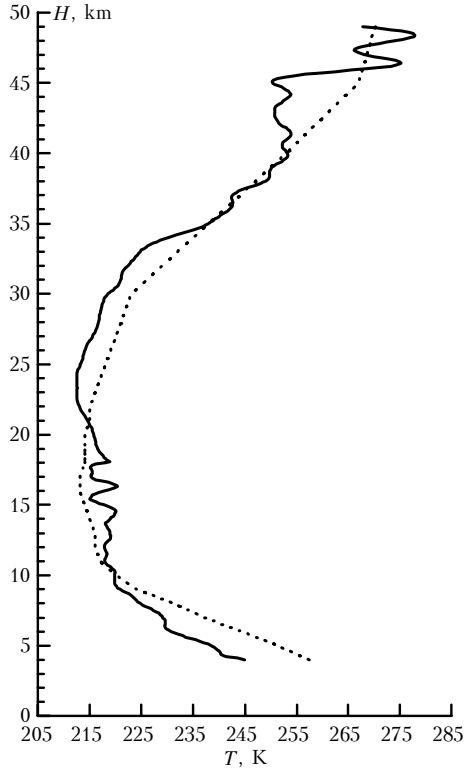

Fig. 6. Vertical profile of the distribution of temperature (solid line) measured on November 20, 1999 as compared with the model profile[22] (dotted line).

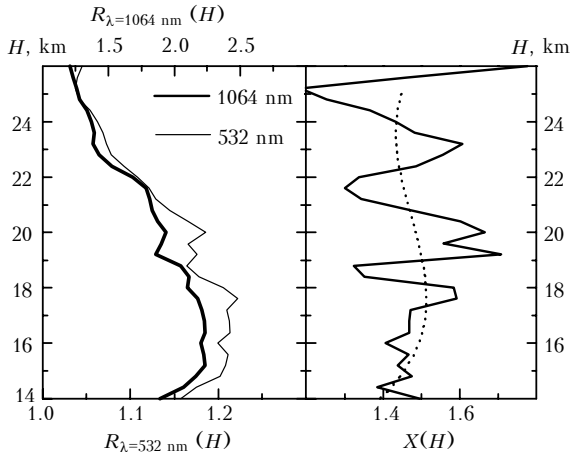

Fig. 7. Vertical profiles of the scattering ratio at the wavelengths of 532 and 1064 nm and the parameter X (polynomial smoothing is shown by dotted line).

Apart from the active laser channels, the channels of passive spectrophotometric measurements of the direct solar radiation and the scattered radiation at zenith are used at the SLS. Photometric measurements of the twilight sky brightness in the blue-green wavelength range make it possible to obtain the data on the total content and vertical distribution of the nitrogen dioxide (VD NO_2).[7] Nitrogen dioxide is one of the most active photochemical components of the stratosphere, which plays principal role in the catalytic ozone cycles. The recorded profiles of nitrogen dioxide for morning and evening twilight with typical maxima at 25–30 km[8] are shown as an example in Fig. 8. Finally, regular measurements of the total ozone content (TOC) are carried out by means of an M–124 ozonometer. The time series of the deviations of monthly mean TOC values from the long-term norm obtained at the SLS since January 1994 till now is shown in Fig. 9. The series is characterized by the statistically significant positive trend.

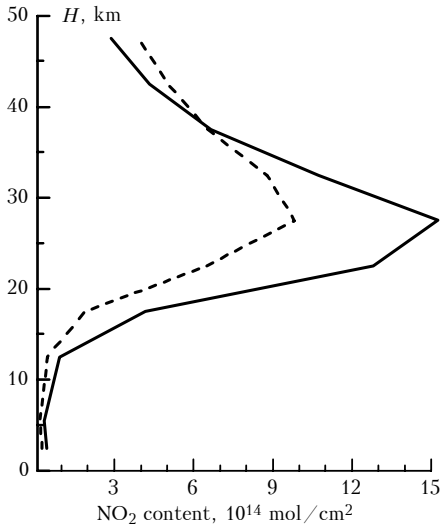

Fig. 8. Vertical distribution of nitrogen dioxide from the data of morning (dotted line) and evening (solid line) measurements on July 12, 1999.

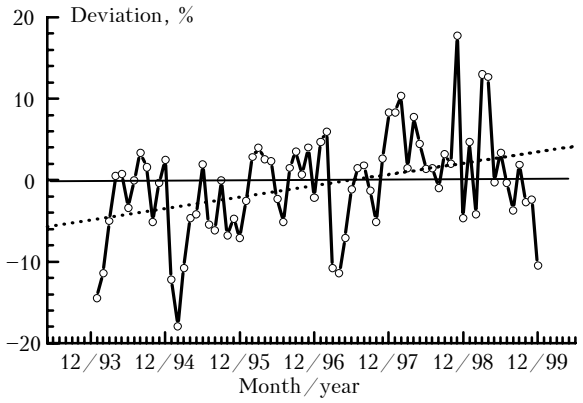

Fig. 9. Time behavior of the deviations of monthly mean values of the total ozone content since January 1994 until December 1999 from the long-term norm and the linear trend of this series.

The experimental data obtained by all SLS channels are regularly added to the common database. The database specification is presented in Table 2. Let us note that the list of the parameters measured at the SLS by only optical methods is necessary and sufficient for description of the principal processes of the ozonosphere transformation.

Factors of photochemical transformation have an effect on the joint variability of VDO, VD NO_2 and VDT in the stratosphere.[8] The effect of atmospheric dynamics is well seen in spatiotemporal variations of all measured parameters that have well pronounced inhomogeneous geographical and altitude distributions. New altitude distributions of the measured parameters are formed due to the horizontal and vertical motions with partial keeping the previous distributions along the motion path. Thus, the joint analysis of variability of all measured parameters makes it possible to determine which air masses and which dynamic processes make up the basis of the observed variations of the ozonosphere.

Typical example of the large-scale advection (invasion) of a cool arctic air mass with high ozone content and typical ozone maximum in the lower stratosphere to the midlatitudes is shown in Fig. 10. Decrease of the ozone content and accompanied adiabatic increase of temperature in the middle stratosphere display the downward motion in the flux divergence zone.

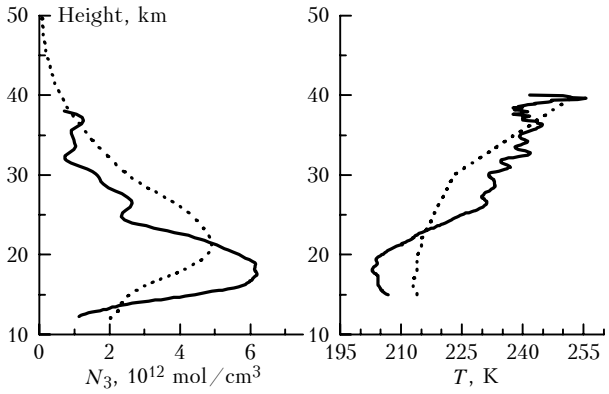

Fig. 10. Vertical profiles of VDO and VDT measured on March 1, 1999 at the invasion of cool arctic air mass (line designations are the same as in Figs. 5 and 6).

Table 2. Characteristic of the experimental database of Siberian Lidar Station

Parameter	Starting year of the time series	Amount of data in the time series	Notes
Total aerosol backscattering coefficient at the wavelength of 532 nm in the height range 10–30 km	1986	About 150 decade-mean values	
Aerosol vertical distribution (based on the data on the optical characteristics of aerosol particles at the wavelength of 532 nm) in the height range 10–30 km	1986	More than 450 nighttime mean profiles	The series also includes the data of episodic measurements at the wavelength of 510 nm
Vertical distribution of the ozone (number density of molecules) in the height range 10–30 (50) km	1989	More than 300 nighttime mean profiles	
Vertical distribution of aerosol (based on the data on the optical characteristics of aerosol particles at the wavelengths of 353, 683, and 1064 nm) in the height range 10–30 km	1991	About 150 nighttime mean profiles	Episodic measurements
Total ozone content	1993	6-year series of the daytime mean values	Regular daily measurements by means of the M–124 ozonometer
Vertical distribution of temperature in the height range 10–50 km	1994	About 200 nighttime mean profiles	
Vertical distribution and total content of nitrogen dioxide	1995	4-year series of twilight measurements	Regular automated measurements in the morning and evening

As is seen from Table 2, the series of experimental data were obtained at the SLS during many years, including both the periods of background (unperturbed) state of the ozonosphere and the periods of perturbation of the ozonosphere by the products of volcanic eruptions, especially the powerful eruption of Mt. Pinatubo. The main results obtained at the SLS during these periods are described in Refs. 9–20. Generalizing them, one can draw the following conclusions:

1. It was shown for the first time that the ozone depression due to the perturbation of the ozonosphere by volcanic aerosol after explosive volcanic eruptions remains for 3–4 years.[19] This depression is caused not only by the heterogeneous interactions of the stratospheric ozone molecules on the volcanic aerosol particle surface, but it is also related to variations of the radiative regime of the stratosphere due to the sharp increase of its albedo because of the appearance of clouds of volcanic origin. It is the factor that is responsible for the long-term depression of the ozonosphere. Distortion of the radiative and heat budget of the stratosphere affect also the balance of the photochemical cycles of stratospheric ozone and the change of the stratospheric circulation. In particular, the meridional transfer in the stratosphere becomes more intensive, especially in winter and spring. It can result in the transport of tropical air masses with small TOC to the midlatitudes.

2. Criteria of the background state of the stratospheric aerosol layer were formulated and argued for the first time.[14] These are based on the absence of significant differences in seasonal (winter and summer) mean profiles of the aerosol stratification and homogeneous aerosol altitude distribution in the stratosphere. The background state of the stratospheric aerosol layer determines the unperturbed background state of the ozonosphere. It is shown that the background state of the ozonosphere is observed only since the second half of 1995 until now.[19] The behavior of the ozonosphere during long time in the 80's and the first half of the 90's was distorted by the effect of volcanic aerosol after eruptions of Mt. Saint-Helen (1981), Mt. El-Chicon (1982), Mt. Del Rouis (1985), Mt. Kelut (1990), and Mt. Pinatubo (1991).

3. Recovery of the stratospheric ozone layer at the boundary of XX and XXI centuries was forecasted for the first time.[20] The gradual and steady increase of TOC observed at the SLS since 1993 retains now in the period of the background state of the ozonosphere. The positive trend of monthly mean values of TOC since January 1994 until December 1999 is $(1.44 \pm 0.41)\%$ per year. Recovery of the ozonosphere, at least in the midlatitudes is now the fact of the global scale.

Let us note for the conclusion that the Siberian Lidar Station created at the Institute of Atmospheric Optics is included into the List of unique Russian scientific-research and experimental setups, that is the recognition of its world level and the unique character of the realized complex approach to the study of the ozonosphere. The author would like to thank the staff of the laboratory of remote spectroscopy of the atmosphere for the titanic efforts when creating the SLS and maintaining regular observations.

Acknowledgments

The work was supported in part by Ministry of Science of Russian Federation at Siberian Lidar Station (No. 01–64) and Russian Foundation for Basic Research (Grant No. 99–05–64943).

References

1. V.V. Zuev, A.V. El'nikov, V.N. Marichev, and S.I. Tsaregorodtsev, Atm. Opt. **2**, No. 9, 841–842 (1989).
2. S.L. Bondarenko, V.D. Burlakov, M.V. Grishaev, et al., Atmos. Oceanic Opt. **7**, No. 11–12, 876-878 (1994).
3. V.V. Zuev, A.V. El'nikov, and V.N. Marichev, Atm. Opt. **4**, No. 2, 175–182 (1991).
4. V.V. Zuev and A.V. El'nikov, Atmos. Oceanic Opt. **5**, No. 10, 681–683 (1992).
5. V.V. Zuev, V.N. Marichev, and S.L. Bondarenko, Atmos. Oceanic Opt. **9**, No. 12, 1026–1029 (1996).
6. V.V. Zuev, B.D. Belan, A.V. El'nikov, et al., Atmos. Oceanic Opt. **5**, No. 6, 379–380 (1992).
7. R.J. McKenzie, P.V. Jonston, C.T. McElroy, J.B. Kerr, J.B. Solomon, J. Geophys. Res. **96**, No. D8, 15499–15511 (1991).
8. V.N. Marichev, V.V. Zuev, M.V. Grishaev, and S.V. Smirnov, in: *Advances in Atmospheric Remote Sensing with Lidar: Selected Papers of the 18th Inter. Laser Radar Conf.*, Berlin, 22–26 July 1996 (Springer–Verlag, Berlin, 1996), pp. 549–552.
9. V.D. Burlakov, A.V. El'nikov, V.V. Zuev, et al., Atmos. Oceanic Opt. **6**, No. 10, 701–706 (1993).
10. V.V. Zuev, M.V. Grishaev, V.N. Marichev, and S.V. Smirnov, Atmos. Oceanic Opt. **10**, No. 10, 732–738 (1997).
11. V.D. Burlakov, A.V. El'nikov, V.V. Zuev, et al., Atmos. Oceanic Opt. **8**, No. 10, 813–816 (1995).
12. V.V. Zuev, V.D. Burlakov, A.V. El'nikov, and S.V. Smirnov, Atmos. Oceanic Opt. **9**, No. 12, 1015–1018 (1996).
13. V.V. Zuev, A.V. El'nikov, and V.N. Marichev, Atmos. Oceanic Opt. **11**, No. 12, 1134–1138 (1998).
14. V.V. Zuev, A.V. El'nikov, and V.D. Burlakov, Atmos. Oceanic Opt. **12**, No. 3, 257–264 (1999).
15. V.N. Marichev, V.V. Zuev, P.A. Khryapov, et al., Atmos. Oceanic Opt. **12**, No. 5, 412–417 (1999).
16. V.V. Zuev, V.N. Marichev, and S.V. Smirnov, Atmos. Oceanic Opt. **12**, No. 10, 864–872 (1999).
17. V.V. Zuev, V.D. Burlakov, and A.V. El'nikov, J. Aerosol Sci. **29**, No. 10, 1179–1187 (1998).
18. V.V. Zuev and S.V. Smirnov, Ivz. Vyssh. Uchebn. Zaved. SSSR, Ser. Fizika **41**, No. 9, 75–82 (1998).
19. V.V. Zuev, V.N. Marichev, and S.V. Smirnov, Izv. Akad. Nauk, Fizika Atmos. Okeana. **35**, No. 5, 1–10 (1999).
20. V.V. Zuev, Atmos. Oceanic Opt. **11**, No. 12, 1168–1169 (1998).
21. A.J. Krueger and R.A. Minzner, J. Geophys. Res. **81**, 4477–4481 (1976).
22. V.E. Zuev and V.S. Komarov, *Statistical Models of Temperature and Gaseous Components of the Atmosphere* (Gidrometeoizdat, Leningrad, 1986), 264 pp.